Analyst

ROYAL SOCIETY OF CHEMISTRY

PAPER

View Article Online
View Journal | View Issue

Cite this: *Analyst*, 2022, **147**, 3464

Detection of paracetamol binding to albumin in blood serum using 2D-IR spectroscopy†

Samantha H. Rutherford, *[a] Gregory M. Greetham,[b] Michael Towrie,[b] Anthony W. Parker,[b] Soheila Kharratian,[c,d] Thomas F. Krauss,[d] Alison Nordon,[e] Matthew J. Baker[a,f] and Neil T. Hunt[c]

Received 13th June 2022,
Accepted 9th July 2022

DOI: 10.1039/d2an00978a

rsc.li/analyst

Binding of drugs to blood serum proteins can influence both therapeutic efficacy and toxicity. The ability to measure the concentrations of protein-bound drug molecules quickly and with limited sample preparation could therefore have considerable benefits in biomedical and pharmaceutical applications. Vibrational spectroscopies provide data quickly but are hampered by complex, overlapping protein amide I band profiles and water absorption. Here, we show that two-dimensional infrared (2D-IR) spectroscopy can achieve rapid detection and quantification of paracetamol binding to serum albumin in blood serum at physiologically-relevant levels with no additional sample processing. By measuring changes to the amide I band of serum albumin caused by structural and dynamic impacts of paracetamol binding we show that drug concentrations as low as 7 μM can be detected and that the availability of albumin for paracetamol binding is less than 20% in serum samples, allowing identification of paracetamol levels consistent with a patient overdose.

Introduction

The interaction of drug molecules with proteins in the blood stream is of relevance to applications ranging from biomedical analysis and diagnostics to drug metabolism and pharmacokinetics (DMPK).[1,2] The degree to which drug molecules bind to serum proteins influences therapeutic efficacy and can determine levels of toxicity in the case of an overdose. Designing analytical protocols to measure bound drug fractions *in situ* is challenging because biofluids contain proteins, carbohydrates, fatty acids and minerals among other constituents.[3–5] As well as making isolation of specific protein binding events difficult, the complex chemical environment can modulate the binding profiles of serum proteins, for example *via* allosteric effects. Thus, the ability to observe intermolecular interactions *in vivo* directly will provide new insight that is of both practical and fundamental value.

Infrared (IR) absorption spectroscopies provide molecular-level insight into complex mixtures but have, to date, failed to detect protein–drug binding in biofluids at clinical levels. This is because water (H_2O) absorptions overlap strongly with the protein amide I band, while drug binding causes only subtle changes to this band, further hampering detection of protein–drug binding.[6] In contrast, two-dimensional infrared (2D-IR) spectroscopy has proven the ability to measure the protein content of biofluids.[7] The amide I band provides a 2D-spectral signature linked to protein secondary structure,[8,9] while the non-linear nature of the 2D-IR experiment suppresses interference from H_2O absorptions.[7] 2D-IR signals have also been shown to be sensitive to protein binding in solution,[6,10,11] suggesting that extension to interactions with serum proteins *in vivo* is feasible. Furthermore, the small sample volumes (<10 μL) needed for 2D-IR along with measurement times of a few minutes per sample raise the realistic prospect of future high-throughput screening applications of 2D-IR.[12,13]

Here, we target 2D-IR detection of paracetamol bound to serum albumin in blood serum at clinically relevant concentrations. Paracetamol is the most common drug consumed in the UK and accounts for ~50% of all drug related hospital admissions.[14] Emergency departments in the UK see on average ~100 000 patients presenting with a paracetamol overdose annually, with around half requiring hospital admission.[14–16] While it is the free drug that is thought to be

[a]*WestCHEM, Department of Pure and Applied Chemistry, University of Strathclyde, Technology and Innovation Centre, 99 George Street, Glasgow, G1 1RD, UK. E-mail: samantha.hume-rutherford@strath.ac.uk*
[b]*STFC Central Laser Facility, Research Complex at Harwell, Rutherford Appleton Laboratory, Harwell Campus, Didcot, OX11 0QX, UK*
[c]*Department of Chemistry and York Biomedical Institute, University of York, Heslington, York, YO10 5DD, UK*
[d]*School of Physics, Engineering and Technology and York Biomedical Research Institute, University of York, Heslington, York, YO10 5DD, UK*
[e]*WestCHEM, Department of Pure and Applied Chemistry and CPACT, University of Strathclyde, 295 Cathedral Street, Glasgow, G1 1XL, UK*
[f]*Dxcover Ltd, Suite RC534, 204 George Street, Glasgow, G1 1XL, UK*
† Electronic supplementary information (ESI) available. See DOI: https://doi.org/10.1039/d2an00978a

primarily responsible for toxic effects, the bound portion acts as a reservoir, releasing the drug in order to maintain an equilibrium of the bound-unbound fractions making it equally important to have knowledge of the bound fraction from a clinical perspective.[17]

Conventional analytical methods used to determine drug concentrations in blood serum employ laboratory-based assays that are only able to target the free drug fraction or the total level *via* protein dissociation.[18–20] Although reliable, these methods typically produce results hours or days after blood collection, leading to delays in decisions and treatments and, potentially, to poorer outcomes and elevated costs associated with longer patient stays in hospital.[21,22] Quicker analytical methods would allow earlier diagnosis, thus patient treatments and discharge from hospital can be managed in a timely manner. Emerging methods using electrochemical finger-prick tests have produced promising results for measuring free paracetamol levels in whole blood, but rapid access to the protein-bound drug concentration in serum remains challenging.[19]

Paracetamol is known to bind to serum albumin,[23] the most abundant serum protein. Serum albumin primarily functions as a carrier protein, binding a variety of substrates and so plays a critical role in the pharmacokinetics of drugs.[4,17,24,25] Although the structure of albumin is known, its binding behaviour is complex. It features at least two drug-binding sites (Sudlow I & II) and seven fatty acid binding sites, occupation of which can allosterically affect binding at the Sudlow sites.[26,27] By adding paracetamol to serum samples spanning the normal clinical range for paracetamol from trace amounts to levels associated with potential hepatotoxicity,[19,28] we used 2D-IR to identify spectroscopic changes in the amide I band of serum albumin and compared the changes to known binding behaviours, demonstrating the ability to detect protein-bound paracetamol at clinical concentrations and introducing a generalised approach for studying drug binding to serum proteins *in vivo.*

Experimental

Sample preparation

Pooled equine serum and paracetamol (Acetaminophen) were obtained from Sigma Aldrich and used without further purification. To establish the albumin (molecular weight; ~66 500 g mol^{-1}) content of the equine blood serum, serum samples were sent to Glasgow School of Veterinary Medicine for standard laboratory testing and the total serum albumin concentration was measured to be 30 mg mL^{-1} (0.45 mM) using the Bromocresol green assay method.[29]

To study the spectroscopy of serum samples at a range of drug concentrations, powdered paracetamol (molecular weight; 151 g mol^{-1}) was spiked into the pooled equine serum at a concentration of 1.8 mM, creating a 4 : 1 molar ratio (1.8 : 0.45 mM) of paracetamol to the serum albumin. This sample was left overnight to maximise probability of drug–protein binding. Serial dilutions were created from the 4 : 1 solution by adding additional pooled serum, maintaining a consistent albumin concentration of 0.45 mM throughout. A total of 10 samples were created (Table 1) with the lowest concentration of paracetamol at 7 μM having a 0.01 : 1 drug : protein molar ratio. These samples span the clinically relevant range of paracetamol after a typical oral dose,[28] from trace amounts to levels associated with potential hepatotoxicity, defined as serum levels at or above 1.323 mM and 43.1 μM at 4 h and 24 h post ingestion respectively.[19]

Additionally, a paracetamol control sample was produced by dissolved the paracetamol at a concentration of 10 mg mL^{-1} (66 mM) in a Tris buffer, in H_2O, at a pH of 7.5, to mimic the serum pH.

2D-IR spectroscopy

2D-IR spectra were recorded using the LIFEtime laser spectrometer at the STFC Central Laser Facility using the Fourier Transform 2D-IR technique. This approach utilises a sequence of three mid-IR laser pulses arranged in the pseudo pump–probe geometry, which has been described previously.[12,30] Mid-IR pulses with a central frequency of 1650 cm^{-1} were employed with a temporal duration of <200 fs and a bandwidth of ~100 cm^{-1}. Two spectra were collected per sample at two different waiting times (T_w) of 250 fs and 5 ps between the pump and probe pulses using a parallel pump–probe polarization. The 250 fs waiting time has been shown to minimise the water signal relative to that from the protein content of the serum, and the 5 ps waiting time is utilised in the pre-processing steps.[31] The acquisition time for each waiting time spectrum is 60 s. Each measurement was made in triplicate using identical sample conditions.

To measure IR and 2D-IR spectra in water using transmission mode, the sample thickness was carefully controlled to avoid saturation of the δ_{H-O-H} mode of water at 1650 cm^{-1}. Samples were housed between two CaF_2 windows and no spacer was used. The tightness of the sample holder was adjusted to obtain a consistent absorbance of ~0.1 for the $\delta_{OH} + \upsilon_{libr}$ combination mode of water located at 2130 cm^{-1}. Based upon the measured molar extinction coefficient of water, this corresponds to a sample thickness of ~2.75 μm.[7]

Table 1 Summary of paracetamol concentrations. Serum albumin concentration was determined to be of 0.45 mmol dm^{-3} *via* standard laboratory testing (ESI†). Samples will be referred to as ^{n}[P] where *n* indicates an *n* : 1 molar ratio of paracetamol to albumin, as shown

Sample	mmol dm^{-3} (mM)	μg mL^{-1}
^{0}[P]	0	0
$^{0.01}$[P]	0.007	1
$^{0.03}$[P]	0.015	2
$^{0.06}$[P]	0.03	4
$^{0.12}$[P]	0.06	9
$^{0.25}$[P]	0.11	17
$^{0.5}$[P]	0.22	34
^{1}[P]	0.45	69
^{2}[P]	0.9	137
^{4}[P]	1.8	275

Data analysis

Prior to analysis, the time domain signal is zero padded and apodised using a Hamming window function prior to Fourier transformation, then pre-processing steps were carried out to remove spectral noise. A polynomial baseline subtraction was performed at each pump frequency and the data was normalised to the water signal using the 2D-IR spectrum obtained at a T_w of 5 ps to account for sample-to-sample variations in path length, as described previously.[31] Noise reduction *via* principal component analysis (PCA) was applied to the spectral dataset.[32] Finally, the spectral region 1600–1700 cm^{-1} on both pump and probe axes was selected for further analysis as this region encapsulates the full amide I band of the serum samples, as shown in Fig. 1.

Principal component analysis (PCA) was used to extract features specific to paracetamol–albumin binding and to discriminate between paracetamol containing samples and neat serum. PCA is an unsupervised multivariate analytical technique that aims to maximise the variance within the dataset, while reducing the data dimensionality.[33,34] The algorithm was used without the addition of built-in scaling, normalisations or mean-centring parameters. Each sample was measured in triplicate, after analysis the results were averaged and standard deviations calculated for each sample concentration.

All 2D-IR spectra were pre-processed and analysed using a custom script written using the statistical analysis software programme, R.[35]

Results and discussion

2D-IR spectra of pooled equine serum samples spiked with paracetamol at concentrations ranging between 7 μM–1.8 mM (Table 1) were obtained (Fig. 1). The negative (red) and positive (blue) peaks present in the 2D-IR spectrum are assigned to the ν = 0–1 and ν = 1–2 transitions of the protein amide I band respectively. As previously described, the dominant diagonal peak at 1650 cm^{-1} in the serum spectrum is due to serum albumin, while the secondary peak at 1635 cm^{-1} is assigned to the globulin proteins.[7]

Applying PCA to 2D-IR spectra has been shown to allow identification of components of mixtures.[36] PCA of the spectra in Fig. 1 revealed two main sources of variance (99.8% of the total). A distinct separation between the serum only sample (Fig. 2(a), black circle) and those containing paracetamol (Fig. 2(a), coloured circles) was observed upon plotting PC1 *versus* PC2, indicating a significant change in the serum spectrum upon addition of paracetamol even from concentrations as low as 7 μM. It is noted that as the data was not mean-centred prior to PCA, PC1 does not centre around zero. Examining these changes in more detail shows that the PC1 score (99.1% variance) remained constant with increasing paracetamol levels (Fig. 2(b)) while there was a notable increase in the PC2 score (0.7% variance, Fig. 2(c)) at small values of [P], which flattens at higher concentrations.

The PC1 loadings plot is in close agreement with that of neat serum (Fig. 2(d) and (e), respectively). The PC2 loadings plot (Fig. 2(f)) shows a dominant feature with a pump frequency of 1652 cm^{-1}, which coincides with the albumin amide I band (Fig. 2(e), black and purple dashed traces). An increase in PC2 score with increasing [P] indicates changes in the spectrum consistent with a reduction in albumin α-helix signal (Fig. 2(f), blue arrow), in agreement with the findings of other groups.[26,37] The PC2 loadings also highlight a decrease in the anharmonicity of paracetamol bound albumin (Fig. 2(f), red arrow) as [P] increases. These observations can also be visualised *via* slices through the 2D-IR spectra at a pump frequency of 1652 cm^{-1} in Fig. 3(b). In contrast to the spectrum of neat serum (black dashed line), a clear shift to lower frequencies and a decrease in the ν = 1–2 mode amplitude is observed with increasing paracetamol concentration (colour traces).

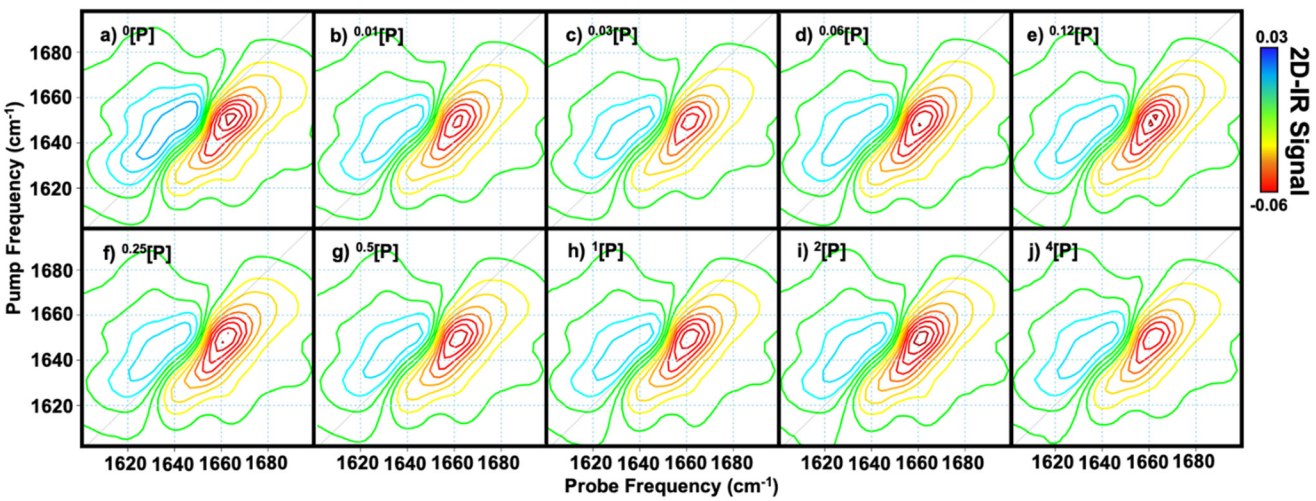

Fig. 1 Pre-processed 2D-IR spectra of serum spiked with paracetamol [P] where (a) neat serum, (b) $^{0.01}$[P], (c) $^{0.03}$[P], (d) $^{0.06}$[P], (e) $^{0.12}$[P], (f) $^{0.25}$[P], (g) $^{0.5}$[P], (h) ^{1}[P], (i) ^{2}[P], (j) ^{4}[P], at waiting time of 250 fs. The figures show the average of three spectra for each sample. Labels denote the molar ratio of drug to serum albumin.

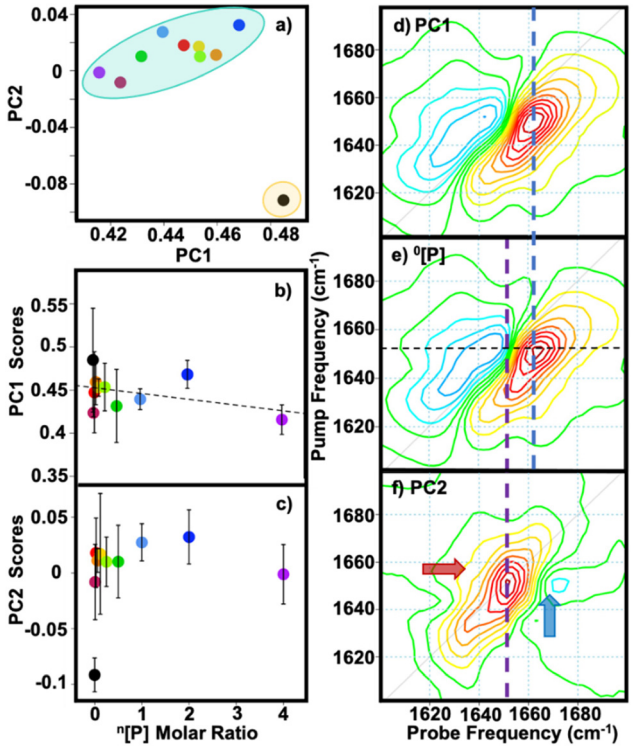

Fig. 2 Principal component analysis (PCA) results for the ^{n}[P] dataset. (a) PC1 *vs.* PC2 scores, yellow and blue ellipses show data separation between ^{0}[P] and those containing [P], respectively. Averaged score results for (b) PC1 and (c) PC2 as a function of [P]. Error bars show 1σ variation. Black dashed line denotes linear fit for PC1. (d) PC1 loadings plot (e) 2D-IR spectrum of ^{0}[P] sample, black dashed line at 1652 cm^{-1} indicates pump slice viewed in Fig. 3 and (f) PC2 loading plot; red and blue arrows highlight lineshapes denoting an increase and reduction in signal, respectively. Blue and purple dashed lines highlight overlap of PC1 and PC2 with ^{0}[P], respectively.

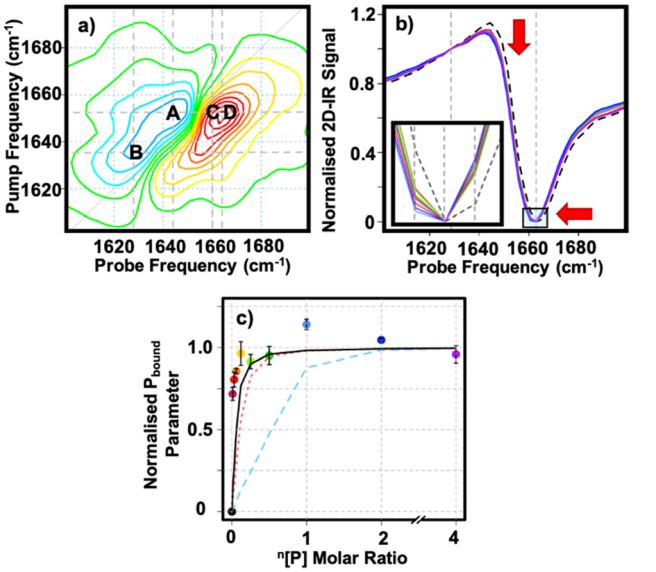

Fig. 3 (a) 2D-IR spectrum of ^{0}[P], letters indicate points used to calculate P_{bound}, horizontal and vertical grey dashed lines mark their frequencies (cm^{-1}), *A* (1652, 1645), *B* (1636, 1629), *C* (1652, 1661), D (1652, 1663). (b) Slices through the 2D-IR spectra of ^{n}[P] at a pump frequency of 1652 cm^{-1}. Black dashed curve denotes ^{0}[P]. For clarity the slice is baselined to 1661 cm^{-1} and normalised to the globulin contribution at 1629 cm^{-1}, indicated by the grey vertical dashed lines. Red arrows indicate directionality of lineshape changes with increasing [P]. Inset shows the negative peak expanded for clarity, denoted by the blue shaded area. Grey vertical dashed lines in inset mark wavenumbers 1661 cm^{-1}, 1663^{-1} and 1665 cm^{-1}. (c) The P_{bound} parameter as a function of ^{n}[P], normalised to the total protein concentration (0.45 mM). Error bars show 1σ variation. Lines show predicted binding curves for different serum albumin availabilities: solid black (10%), dotted red (20%) and dashed blue (100%).

To ascertain that these spectral changes are not attributable to unbound paracetamol, a 2D-IR spectrum was obtained at a concentration of 66 mM, ~40 times greater than the highest levels used in serum experiments, in aqueous buffer (Fig. S1†). Not only was the spectrum of free paracetamol too weak to detect at the levels added to serum samples, but the bands due to paracetamol did not coincide with the changes observed in the serum spectra. We thus assign the PC1 contribution to neat serum (Fig. 2(d and e)) and PC2 to spectral changes to the albumin signal associated with the addition of paracetamol (Fig. 2(f)).

To confirm the assignment of spectral changes due to albumin–paracetamol binding, we compared the spectral changes revealed by PCA with predictions of serum–paracetamol binding based on the known binding constant.[37] To quantify the spectral changes, four data points, A–D, highlighted in Fig. 3(a) were used with the equation:

$$P_{\text{bound}} = \frac{1.8B}{A} \times \frac{C}{D}.$$

The ratio of points *A* and *B* quantifies changes in the albumin ν = 1–2 peak relative to that of the globulin serum fraction, which is invariant with [P] (Fig. 2(f)). A reduction in signal at point A as observed for paracetamol binding, will thus increase this ratio. A previously-determined scaling factor of 1.8 has been applied to account for differences in the molar extinction coefficients of albumin and globulin.[7] Similarly, the ratio of points C and D quantify the shift of the albumin peak to lower probe wavenumbers with increasing [P] (Fig. 3(b)), arising from a change in the anharmonicity of the amide I band of albumin. Plotting the P_{bound} parameter, normalised to the total protein concentration to mimic the drug–protein binding curve (Fig. S2†), as a function of drug concentration (Fig. 3(c)) results in the dependence on [P] shown in Fig. 3(c).

Albumin is reported to have one or two binding sites for paracetamol,[37–39] which correlates well with the fact that our data shows spectral changes saturated at a paracetamol : albumin molar ratio close to unity (Fig. 3(c)). The association constant for paracetamol and albumin has been determined to be 1 × 10^4 mol L^{-1}.[37] Comparing the normalised P_{bound} parameter to the expected concentration of paracetamol : albumin complex for a given [P] based on an albumin concentration of 0.45 mM, gives poor agreement with the experimental data (blue dashed line (Fig. 3(c)). However, this ana-

lysis assumes that all of the albumin in our samples is available for binding. By contrast, studies over a range of albumin and paracetamol concentrations suggests that only a small fraction (10–20%) of the albumin is available to bind paracetamol.[23,40] Changing the model to reflect this reduced protein availability (10% solid black; 20% red dotted traces, Fig. 3(c)) gives much better agreement with the paracetamol binding parameter, showing that our data is consistent with available literature.[23,40]

Conclusions

We conclude that 2D-IR spectral analysis of paracetamol-spiked blood serum samples permits the quantification of albumin bound paracetamol content from concentrations as low as 1 μg mL^{-1} (7 μM) up to the point where binding is saturated 69 μg mL^{-1} (0.45 mM). Above these concentrations, 2D-IR is able to show that all of the available albumin is in a bound state and therefore provides a lower limit for total paracetamol concentration, which may be useful under conditions of overdose. It is noteworthy that, by using the amide I band, the detection limit for paracetamol-induced changes to serum is several orders of magnitude lower than would have been possible if detecting free paracetamol using 2D-IR. The large molar extinction coefficient of the amide I band effectively enhances the signal due to paracetamol binding. From a biomedical perspective, it is clear that 2D-IR is capable of measuring the presence of protein-bound paracetamol at concentrations that would be expected to cause toxic effects (43 μM), without directly measuring the free paracetamol concentration. Further work is required to determine whether the spectral changes observed are unique to the paracetamol–albumin interaction or generic albumin binding. Similar changes in spectroscopy, featuring reductions in amide I anharmonic shifts and signal amplitudes have been observed for other systems, and we anticipate that these results will motivate a more detailed study of protein amide I spectroscopy under aqueous conditions, with the caveat that albumin in serum may behave rather differently to that in aqueous solutions as a result of fatty acid concentrations in the former. Overall, we believe that our results serve to demonstrate that 2D-IR spectral analysis can be applied in a matter of seconds and opens up the possibility of 2D-IR screening applications in the biomedical arena.

With regard to the use of 2D-IR for general DMPK applications, characterisation of the spectral impact of albumin binding for any small molecule could be achieved following this protocol. The effectiveness of the 2D-IR approach will depend upon the spectral effect of binding and the effective concentrations of the drug and the binding constant, however, the potential for further development of the method is clear. When combined with our methodologies,[7,31] the application of 2D-IR to detect and understand drug–protein complexes in serum is highlighted, making significant progress and allowing rapid, non-destructive, label-free and accurate diagnostics *in situ* without the need for any sample preparation or isolation of compounds. The ability to measure directly within blood and its derivatives will enable more effective drug treatments to be developed and advance the understanding of drugs in the human system as well as providing an approach to studying intermolecular structural dynamics *in vivo.*

Data availability

All the data underpinning this publication are openly available from the University of Strathclyde KnowledgeBase at **https://doi.org/10.15129/453a67c8-406c-4854-83ae-de851c4eb019**.

Conflicts of interest

There are no conflicts to declare.

Acknowledgements

Funding from EPSRC (EP/T014318/1 and EP/V047663/1) for this work is gratefully acknowledged. STFC funding for access to the ULTRA suite of spectrometers is also acknowledged. The assistance of Mr James Harvie (University of Glasgow School of Veterinary Medicine) in obtaining the albumin concentration in horse serum samples is gratefully acknowledged.

References

1 J. S. Kang and M. H. Lee, *Korean J. Intern. Med.*, 2009, **24**, 1–10.
2 Y. Li, Q. Meng, M. Yang, D. Liu, X. Hou, L. Tang, X. Wang, Y. Lyu, X. Chen, K. Liu, A. M. Yu, Z. Zuo and H. Bi, *Acta Pharm. Sin. B*, 2019, **9**, 1113–1144.
3 G. J. van der Vusse, *Drug Metab. Pharmacokinet.*, 2009, **24**, 300–307.
4 A. A. Spector, *J. Lipid Res.*, 1975, **16**, 165–179.
5 M. J. Baker, S. R. Hussain, L. Lovergne, V. Untereiner, C. Hughes, R. A. Lukaszewski, G. Thiéfin and G. D. Sockalingum, *Chem. Soc. Rev.*, 2016, **45**, 1803–1818.
6 D. Shaw, R. Hill, N. Simspon, F. Husseini, K. Robb, G. M. Greetham, M. Towrie, A. W. Parker, D. Robinson, J. Hirst, P. A. Hoskisson and N. Hunt, *Chem. Sci.*, 2017, **8**, 8384–8399.
7 S. Hume, G. Hithell, G. M. Greetham, P. M. Donaldson, M. Towrie, A. W. Parker, M. J. Baker and N. T. Hunt, *Chem. Sci.*, 2019, **10**, 6448–6456.
8 Z. Ganim, H. S. Chung, A. W. Smith, L. P. Deflores, K. C. Jones and A. Tokmakoff, *Acc. Chem. Res.*, 2008, **41**, 432–441.
9 C. R. Baiz, C. S. Peng, M. E. Reppert, K. C. Jones and A. Tokmakoff, *Analyst*, 2012, **137**, 1793–1799.
10 D. J. Shaw, K. Robb, B. V. Vetter, M. Tong, V. Molle, N. T. Hunt and P. A. Hoskisson, *Sci. Rep.*, 2017, **7**, 1–7.

11 L. Minnes, D. J. Shaw, B. P. Cossins, P. M. Donaldson, G. M. Greetham, M. Towrie, A. W. Parker, M. J. Baker, A. J. Henry, R. J. Taylor and N. T. Hunt, *Anal. Chem.*, 2017, **89**, 10898–10906.
12 P. M. Donaldson, G. M. Greetham, D. J. Shaw, A. W. Parker and M. Towrie, *J. Phys. Chem. A*, 2018, **122**, 780–787.
13 R. Fritzsch, P. M. Donaldson, G. M. Greetham, M. Towrie, A. W. Parker, M. J. Baker and N. T. Hunt, *Anal. Chem.*, 2018, **90**, 2732–2740.
14 NHS, Paracetamol Toxicity Management Guideline, **https://www.northdevonhealth.nhs.uk/wp-content/uploads/2021/01/Paracetamol-Toxicity-Management-Guideline.pdf**, (accessed 22 March 2020).
15 D. N. Bateman, R. Carroll, J. Pettie, T. Yamamoto, M. E. M. O. Elamin, L. Peart, M. Dow, J. Coyle, K. R. Cranfield, C. Hook, E. A. Sandilands, A. Veiraiah, D. Webb, A. Gray, P. I. Dargan, D. M. Wood, S. H. L. Thomas, J. W. Dear and M. Eddleston, *Br. J. Clin. Pharmacol.*, 2014, **78**, 610–618.
16 D. Casey, G. Geulayov, E. Bale, F. Brand, C. Clements, N. Kapur, J. Ness, A. Patel, K. Waters and K. Hawton, *J. Affective Disord.*, 2020, **276**, 699–706.
17 J. J. Vallner, *J. Pharm. Sci.*, 1977, **66**, 447–465.
18 P. Soysa and S. Kolambage, *J. Natl. Sci. Found. Sri Lanka*, 2010, **38**, 131–137.
19 N. Wester, B. F. Mikladal, I. Varjos, A. Peltonen, E. Kalso, T. Lilius, T. Laurila and J. Koskinen, *Anal. Chem.*, 2020, **92**, 13017–13024.
20 L. S. Jensen, J. Valentine, R. W. Milne and A. M. Evans, *J. Pharm. Biomed. Anal.*, 2004, **34**, 585–593.
21 C. Dale, A. A. M. Aulaqi, J. Baker, R. C. Hobbs, M. E. L. Tan, C. Tovey, I. A. L. Walker and J. A. Henry, *QJM - Mon. J. Assoc. Physicians*, 2005, **98**, 113–118.
22 D. W. Roberts, W. M. Lee, J. A. Hinson, S. Bai, C. J. Swearingen, R. T. Stravitz, A. Reuben, L. Letzig, P. M. Simpson, J. Rule, R. J. Fontana, D. Ganger, K. R. Reddy, I. Liou, O. Fix and L. P. James, *Clin. Gastroenterol. Hepatol.*, 2017, **15**, 555–562.
23 T. P. Milligan, H. C. Morris, P. M. Hammond and C. P. Price, *Ann. Clin. Biochem.*, 1994, **31**, 492–496.
24 U. Kragh-Hansen, *Pharmacol. Rev.*, 1981, **33**, 17–53.
25 S. Baroni, M. Mattu, A. Vannini, R. Cipollone, S. Aime, P. Ascenzi and M. Fasano, *Eur. J. Biochem.*, 2001, **268**, 6214–6220.
26 M. Fasano, S. Curry, E. Terreno, M. Galliano, G. Fanali, P. Narciso, S. Notari and P. Ascenzi, *IUBMB Life*, 2005, **57**, 787–796.
27 E. S. Krenzel, Z. Chen and J. A. Hamilton, *Biochemistry*, 2013, **52**, 2382.
28 A. Richter and S. E. Smith, *Br. J. Clin. Pharmacol.*, 1974, **1**, 495–498.
29 J. R. Harding and J. W. Keyser, *Proc. Assoc. Clin. Biochem.*, 1968, **5**, 51–53.
30 G. M. Greetham, P. M. Donaldson, C. Nation, I. V. Sazanovich, I. P. Clark, D. J. Shaw, A. W. Parker and M. Towrie, *Appl. Spectrosc.*, 2016, **70**, 645–653.
31 S. Hume, G. M. Greetham, P. M. Donaldson, M. Towrie, A. W. Parker, M. J. Baker and N. T. Hunt, *Anal. Chem.*, 2020, **92**, 3463–3469.
32 Y. M. M. Babu, M. V. Subramanyam and M. G. Prasad, *Signal Image Processing: An International Journal (SIPIJ)*, 2012, **3**, 236–244.
33 R. Bro and A. K. Smilde, *Anal. Methods*, 2014, **6**, 2812–2831.
34 S. H. Rutherford, A. Nordon, N. T. Hunt and M. J. Baker, *Chemom. Intell. Lab. Syst.*, 2021, **217**, 104408.
35 R. Team, *R Found. Stat. Comput*.
36 S. H. Rutherford, G. M. Greetham, P. M. Donaldson, M. Towrie, A. W. Parker, M. J. Baker and N. T. Hunt, *Anal. Chem.*, 2021, **93**, 920–927.
37 P. Daneshgar, A. A. Moosavi-Movahedi, P. Norouzi, M. R. Ganjali, A. Madadkar-Sobhani and A. A. Saboury, *Int. J. Biol. Macromol.*, 2009, **45**, 129–134.
38 P. Daneshegar, A. A. Moosavi-Movahedi, P. Norouzi, M. R. Ganjali, M. Farhadic and N. Sheibani, *J. Braz. Chem. Soc.*, 2012, **23**, 315–321.
39 A. Sułkowska, B. Bojko, J. Równicka and W. W. Sułkowski, *J. Mol. Struct.*, 2006, **792–793**, 249–256.
40 M. E. Morris and G. Levy, *J. Pharm. Sci.*, 1984, **73**, 1037–1041.